CONCEPTS & SYNTHESIS
EMPHASIZING NEW IDEAS TO STIMULATE RESEARCH IN ECOLOGY

Ecological Monographs, 85(3), 2015, pp. 353–371

A dynamic energy budget for the whole life-cycle of holometabolous insects

Ana L. Llandres,[1,6] Gonçalo M. Marques,[2,3] James L. Maino,[4] S. A. L. M. Kooijman,[5] Michael R. Kearney,[4] and Jérôme Casas[1]

[1]*Institut de Recherche sur la Biologie de l'Insecte, Université de Tours, UMR CNRS 635, Avenue Monge-Parc Grandmont, 37200, Tours, France*
[2]*CIMO–Mountain Research Center, Instituto Politécnica de Bragança, Campus de Santa Apolónia, Apartado 1172, 5301-855 Bragança, Portugal*
[3]*MARATEC–Marine, Environment and Technology Center, Instituto Superior Técnico, Universidade de Lisboa, Avenida Rovisco Pais 1, 1049-001 Lisboa, Portugal*
[4]*School of Biosciences, University of Melbourne, Victoria 3010 Australia*
[5]*Department of Theoretical Biology, Vrije Universiteit, NL-1981 Amsterdam, The Netherlands*

Abstract. Alterations of the amount and quality of food consumed during ontogeny can affect different life-history traits, such as growth rate, developmental time, survival, adult size, and fitness. Understanding the dynamics of such metabolic and energetic pathways and investments is particularly challenging in the case of holometabolous insects due to their strikingly different life stages. We show how whole life-cycle energy and mass budgets can be achieved for holometabolic insects through dynamic energy budget (DEB) theory, permitting the fate of acquired and stored nutrients to be followed over a complete life-cycle. We applied the DEB theory to model the whole life-cycle energetics of an endoparasitic wasp, *Venturia canescens* (Hymenoptera: Ichneumonidae). Data on embryo, larval, and pupal dry mass, imago longevity, and fecundity were used for assessing the goodness of fit of the model. Our model predicted the growth curves of the larval and pupal stages, the number of eggs laid by the imago through time, and lifespan events, such as the different developmental times of the parasitoid. The model enabled us to distinguish and follow the energy invested in eggs through income and capital reserves. The mechanisms leading to the double costs of being small (a shorter life under starving conditions and fewer eggs) were identified by running the model for varying amounts of food eaten early in life, according to host sizes. The final larval instar harvests around 60 times the energy of a recently hatched larva. Around 90% of this energy is then used during pupation to build the structure of the imago and to pay maintenance. Imagoes, therefore, emerge with only a small percentage of the energy stored by the last instar larvae. Our study shows that, despite being small, this percentage of energy stored during the parasitoid development has a great impact on adult fitness, the loss of which cannot be compensated for by a rich adult environment. Our model is generic and has applications for a wide range of applied and theoretical questions about insect energetics, from population dynamics in multitrophic systems to responses to climate change and life-history strategies.

Key words: capital resources; energy acquisition; energy budgets; fitness; holometabolous insects; income resources; nutrient dynamics; parasitoids; resource allocation; Venturia canescens.

Introduction

Alterations of the amount and quality of food consumed during life have wide-ranging effects on many life-history characteristics of animals such as growth rate, developmental time, survival, adult size, and fitness (Joern and Behmer 1997, Taborsky 2006, Barrett et al. 2009). Fitness depends not only on resource uptake but also on the allocation of these resources to various life-history functions (Sibly and Calow 1986, Heino and Kaitala 1999). The field of ecological energetics integrates metabolic processes and constraints, both internal

Manuscript received 26 May 2014; revised 30 January 2015; accepted 4 February 2015. Corresponding Editor: J. A. Rosenheim.
[6] Corresponding author. E-mail: anallandres@gmail.com

and external to the organism, to trace the quantities of nutriments and energy ingested and their allocation to fitness enhancing processes (Tomlinson et al. 2014). The models used in ecological energetics are diverse in their nature and contexts, but abide by common principles, such as homeostasis and the conservation of energy (Humphries and McCann 2014). They can range from highly detailed, descriptive functions that are species-specific in their parameters and structure, to more general formulations based on a core set of theoretical assumptions, often involving a higher degree of abstraction (Nisbet et al. 2012).

Current approaches falling on the more formalized and general end of the spectrum include the stoichiometric approach (Elser et al. 2000), the geometric framework of nutrition (Simpson and Raubenheimer 2012), the metabolic theory of ecology (Brown et al. 2004), and the dynamic energy budget theory (DEB; Kooijman 2010). The relative merits of these different approaches and their relationship have been discussed in previous publications and the convergence of these different theories is a vibrant field of research (Nisbet et al. 2012, Maino et al. 2014). The contexts in which models of ecological energetics are applied vary from conservation physiology and biology (Raubenheimer et al. 2012), the characterization of the niche (Kearney et al. 2010*a*), and the structure and stability of food webs (Getz 2011), often in the context of global changes. Metabolic processes are often strongly coupled to the ability of organisms and higher levels of biological organization to adapt to changes, and this is a question at the heart of evolutionary biology (Applebaum et al. 2014). Thus, the energetic view of resource acquisition and allocation spans both ecology and evolution.

Most described species on earth are holometabolous insects, but the impact of acquisition and allocation of resources in this group is challenging to study due to their strikingly different life-stages (Simpson and Raubenheimer 2012). The differences can be so extreme that entire life stages do not feed at all. The pupal stage in all holometabolous insects is exemplary. The imago stage in some Diptera, Lepidoptera, Trichoptera, and Megaloptera do not feed either (Mathavan et al. 1987, Wissinger et al. 2004, Cover and Resh 2008, Rosenheim et al. 2008). For holometabolous insects that do not feed during the imago stage, egg provisioning is fueled through the energy stores accumulated in earlier instars, called capital resources (Jervis et al. 2008). For other insects that feed during the imago stage, the egg provisioning is supplemented by income resources, i.e., energy gained at the imago stage (Jervis et al. 2008). The consequences of resource acquisition and allocation during each life stage of the insect are thus very complex to study as the resources are redistributed between compartments during metamorphosis. The fat body in particular, which has a key nutrient storage function, undergoes a profound transformation during metamorphosis (Larsen 1976, Nelliot et al. 2006, Hoshizaki et al. 2013). The tissue of the fat body dissociates as it is transformed from an organized tissue in the larva to a loose association of individual fat cells during pupation. This phenomenon has been documented in Diptera and Lepidoptera and is likely to be a common phenomenon of holometabolous insects (Larsen 1976, Nelliot et al. 2006, Hoshizaki et al. 2013). Tracing the fate of stored nutrients over a complete life cycle of insects is therefore complex but can be pursued through the existing theoretical framework developed in the field of ecological energetics.

The broad concepts of DEB theory have recently been applied to understand metabolic-scaling phenomena in insects and show that it can capture paradoxical patterns, such as the U-shaped respiration curve during pupation (Maino and Kearney 2014). The advantage of using the DEB approach for understanding energy budgets is that it provides a powerful set of null expectations for the covariation of life-history traits based only on physicochemical constraints. The traditional approach in life-history theory is to assume evolution optimizes traits to maximize life-time reproduction (see Stearns 1992, Roff 2002). Such optimizations must occur within constraints, and DEB theory specifies for particular linkages among life-history traits and their variation with the environment. It provides theoretically grounded predictions for how different life-history traits are related in the context of an organism's energy and mass budget through ontogeny, and also predicts how life-history traits should scale with size, in the absence of any optimality criterion. There is great potential for a fusion of DEB theory with traditional optimality methods (Kearney 2012, Nisbet et al. 2012, Maino et al. 2014).

In this study, we develop a detailed and generic DEB model for holometabolous insects capable of making quantitative predictions of the processes of feeding, growth, development, and reproduction across the entire life cycle. In particular, our model predicts the growth curves of the larval and pupal stages, the number of eggs laid by the imago through time, and different lifespan events, such as the different developmental times of the parasitoid. We use it to consider the energetics of a holometabolous insect, *Venturia canescens* parasitoid (Hymenoptera: Ichneumonidae) and its implications for different life-history traits. This parasitoid species represents a hyperdiverse insect clade and is particularly interesting from an energetic perspective in using both capital- and income-breeding strategies of energy allocation to reproduction. This species will therefore also allow us to consider the carryover effect of nutrition environments experienced by early developmental stages, i.e., capital reserves, and the effect of adult nutrition, i.e., income reserves, on several life-history traits of the parasitoid. Our resultant model is detailed yet generalizable and is suitable for studying the underlying energy demand, utilization, and storage of capital and income reserves over an entire life cycle of holometabolous

TABLE 1. Energy fluxes linked to different metabolic processes present in the standard dynamic energy budget (DEB) model.

Metabolic process	Energy flux	Life stage
Assimilation	$\dot{p}_A = \{\dot{p}_{Am}\} f V^{2/3}$	juv, adl
Mobilization	$\dot{p}_C = E\dfrac{[E_G]\dot{v}/V^{1/3} + [\dot{p}_S]}{\kappa[E] + [E_G]}$	emb, juv, adl
Somatic maintenance	$\dot{p}_S = \dot{p}_M + \dot{p}_T = [\dot{p}_M]V + \{\dot{p}_T\}V^{2/3}$	emb, juv, adl
Growth	$\dot{p}_G = \kappa\dot{p}_C - \dot{p}_S = \kappa\dot{p}_C - \dot{p}_M - \dot{p}_T$	emb, juv, adl
Maturity maintenance	$\dot{p}_J = \dot{k}_J E_H$	emb, juv, adl
Maturation	$\dot{p}_R = (1-\kappa)\dot{p}_C - \dot{p}_J$	emb, juv
Reproduction	$\dot{p}_R = (1-\kappa)\dot{p}_C - \dot{p}_J$	adl

Notes: The standard DEB model identifies three stage transitions with fundamental changes in the energy budget: embryo (em), juvenile (juv), and adult (adl). $[E]$ represents energy density ($[E] = E/V$, J/cm^3), f is the feeding functional response, which can vary between 0 and 1, and $V^{2/3}$ is the biosurface of the animal. For the units and meaning of the DEB parameters, see Table 3.

insects. Furthermore, the formulation of the DEB model for holometabolous insects provides new opportunities to address questions spanning from life-history strategies and climate-change responses in insects to food-web structure and population dynamics of host–parasitoid systems. These are further developed in *Discussion*.

MATERIALS AND METHODS

Standard DEB model

This section briefly describes the standard DEB model that was constructed to model the life cycle of a generic heterotrophic aerobe. A full description of the model can be found in Kooijman (2010). The standard DEB model is a mechanistic model that tracks the energy flow through organisms during their lifespan through development, reproduction, maintenance, and growth.

Life stages, state variables, and energy fluxes.—In the standard DEB model, the life cycle is characterized by three life stages that can be distinguished by their energy fluxes: embryo, juvenile, and adult. An embryo does not assimilate energy from food but relies on stored energy supplies for development (normally called maturation in DEB theory), growth, and maintenance processes. The second stage is the juvenile stage. The transition between the embryo and juvenile stage occurs once the individual has achieved a particular threshold of energy invested in development. At this point, the individual is sufficiently complex to start feeding and uses the energy acquired through food for continuing its development, growth, and maintenance, but it does not allocate energy to reproduction. Further investment in development leads to a second transition, which is the transition between the juvenile and the adult stage. When the organism becomes an adult, it stops allocating energy to development and redirects this energy to the formation of gametes.

The model has four state variables (units are given in parentheses): E(J), V(cm^3), E_H(J) for embryos and juveniles, and E_R(J) for adult individuals. E is the amount of energy in reserve, V is the volume of structural mass, E_H is the level of maturity, i.e., total energy invested in maturation, which increases throughout the animal's development until adulthood. DEB theory links the occurrence of metabolic switches (e.g., when assimilation is initiated, when allocation to maturation is redirected to reproduction, etc.) to the level of maturity, i.e., the set of regulation systems that control metabolic performance (Kooijman 2010). The building up of maturity costs energy, and maturity is quantified as the cumulated energy or amount of reserve that is invested in maturity. Energy invested in maturation cannot be stored and so is dissipated as heat. In this way, the level of maturity controls life-stage transitions: E_H^b indicates the onset of assimilation when the embryo turns into a juvenile and E_H^p the onset of allocation to reproduction when the juvenile turns into adult. For a full explanation of the maturity concept, see Kooijman (2010). For pedagogical purposes, the analogy between this state variable and the manual counter that flight attendants use to count people sitting on an airplane is useful. Pressing the counter button costs energy, which is not stored anywhere but released to the environment. The counter has the same mass and energy after each count. However, the counter stores the information about the number of people it has counted so far, and although the mass is the same, it is arranged in a different manner. As the manual counter, maturity stores information that tells us when the animal experiences metabolic switches. Finally, the state variable E_R is the reproduction buffer, i.e., the amount of energy invested in reproduction by adult individuals that will be converted to eggs. Dynamics of all the four state variables are determined by the energy fluxes, expressed in J/d: $\dot{p}_A$, $\dot{p}_C$, $\dot{p}_S$, $\dot{p}_G$, $\dot{p}_J$, and $\dot{p}_R$ (see Appendix A for definitions). For a detailed specification of the energy fluxes, see Table 1.

Model functioning: dynamics of the state variables.—In the standard DEB model, food uptake is assumed to follow a type II functional response according to Holling (1959). The animal ingests food and assimilates it with a certain assimilation efficiency given by the parameter κ_x. The ingested food is converted into assimilates that are added to the reserve, E, through the relationship $\dot{p}_A = \kappa_x \dot{p}_x$. Therefore, an organism that

Table 2. Equations describing the dynamics of the state variables.

State variable	Equation
Reserve (E)	$\frac{dE}{dt} = \dot{p}_A - \dot{p}_C$
Structure (V)	$\frac{dV}{dt} = \frac{\dot{p}_G}{[E_G]}$
Maturation (E_H)	$\frac{dE_H}{dt} = \dot{p}_R$ if $E_H < E_H^p$
Reproduction buffer (E_R)	$\frac{dE_R}{dt} = \dot{p}_R$ if $E_H = E_H^p$

assimilates energy from food changes the reserve compartment according to an input $\dot{p}_A$ and an output $\dot{p}_C$, which represents the flux of mobilized reserve that fuels the animal energetic needs. A fixed proportion, κ, of the energy mobilized from the reserve is allocated to somatic maintenance and growth, and the rest, $(1 - \kappa)$, is allocated to maturity maintenance and to maturation/reproduction in juvenile/adults, respectively (Appendix A). This split is called the kappa rule and gives us information on the proportion of energy invested in soma vs. development/reproduction. Adult individuals convert the reproduction buffer, E_R, to eggs with a constant reproduction efficiency, κ_R. As maximum size differs among species, a zoom factor, z, is used to compare physical parameters of an animal to a reference animal of maximum length, L_m^{ref}, of 1 cm (Kooijman 2010). The shape coefficient δ_M converts physical length L_W to structural length L by the equation $L = L_w\delta_M$. The structural volume is the structural length cubed, thus $V = (L_w\delta_M)^3$. The dynamics of the state variables are specified in Table 2 and the primary DEB parameters in Table 3.

Study species

Venturia canescens is a solitary endoparasitoid that parasitizes several larval instars of different pyralid moth species that are pests of stored food products (Salt 1976). This parasitoid species is synovigenic and produces large numbers of small, hydropic eggs, i.e., eggs that absorb nutrients from the host (Fisher 1971, Ohbayashi et al. 1994, Jervis et al. 2001). The larva develops inside the host by feeding from its hemolymph and tissues. The imagoes emerge with some of their total egg complement matured and then feed on sugar (Harvey et al. 2001). There is no egg resorption in this species (Eliopoulos et al. 2003).

A generic DEB model for holometabolous insects

We present the extensions of the DEB model for holometabolous insects. These extensions include (1) the incorporation of four life stages (embryo, larvae, pupa, and imago), (2) allocation to reproduction and a constant maturation level at the larval stage, (3) an energetic threshold for pupation, (4) a resetting of maturation at pupation for the building up of the imaginal structure, (5) a transformation of larval structure to reserve during pupation, (6) the incorporation of egg maturation during the pupal stage, (7) a dual allocation of energy to reproduction and maintenance in the adult insect, and (8) a change in shape between life stages and its concomitant metabolic acceleration. More specific extensions to *V. canescens* parasitoid species are explained in *Materials and methods: Particularities for* Venturia canescens *parasitoids* and include (9) the splitting of the embryonic life into two stages to capture the hydropic nature of its eggs, (10) the production of cocoon silk by the larva, and (11) the mixing of nutrients from capital and income sources in eggs at the adult stage.

Stages and associated parameters.—A full schematic representation of each life stage modeled in *Venturia canescens* is shown in Fig. 1. It is important to highlight that this figure includes not only the modifications incorporated for the generic model built for holometabolous insects but also the specific modifications incor-

Table 3. List of DEB parameters.

Parameter	Description	Units
Primary parameters		
$\{\dot{F}_m\}$	maximum surface-area specific searching rate	$1{\cdot}cm^{-2}{\cdot}d^{-1}$
κ_X	assimilation efficiency	
$\{\dot{p}_{Am}\}$	maximum surface-area specific assimilation rate	$J{\cdot}cm^{-2}{\cdot}d^{-1}$
f	Holling type II scaled functional response	
$[E_G]$	volume-specific cost of structure	J/cm^3
υ	energy conductance	cm/d
$[\dot{p}_M]$	volume-specific somatic maintenance	$J{\cdot}d^{-1}{\cdot}cm^{-3}$
κ	fraction of mobilized reserve allocated to soma	
$\dot{k}_J$	maturity maintenance rate coefficient	d^{-1}
E_H^b	maturity threshold from embryo to juvenile	J
E_H^p	maturity threshold from juvenile to adult	J
κ_R	fraction of the reproduction buffer fixed into eggs	
z	zoom factor	
δ_M	shape correction coefficient	
Ageing parameters		
$\ddot{h}_a$	Weibull ageing acceleration	d^{-2}
s_G	Gompertz stress coefficient	

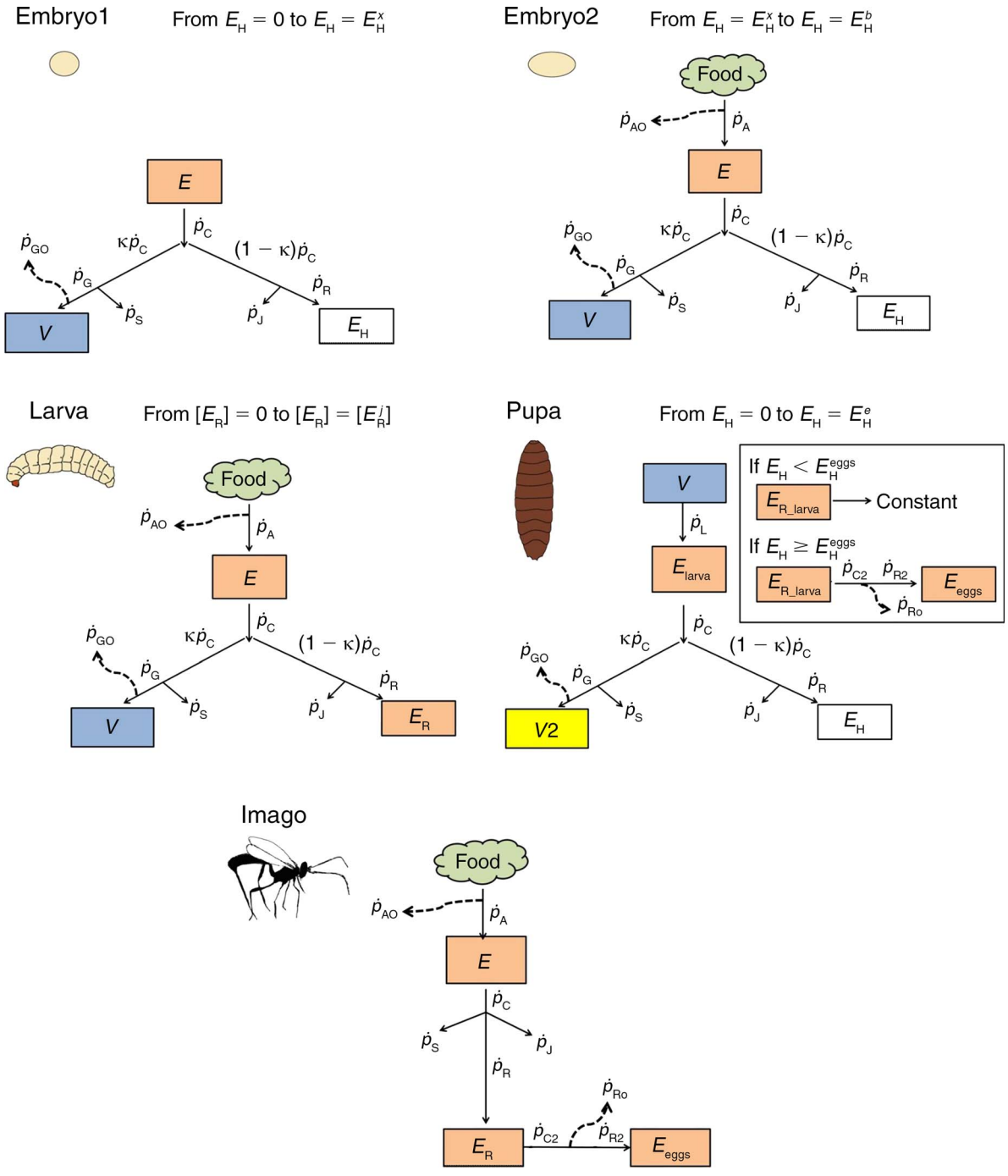

FIG. 1. Representation of the dynamic energy budget (DEB) for the different life stages of the DEB model built for *Venturia canescens* parasitoids. The colors are visual aids facilitating the recognition of variables over ontogeny: food, reserve (E), reproduction buffer (E_R), egg buffer (E_{eggs}), structure (V), and maturation (E_H). The model incorporates five life stages: embryo1, embryo2, larva, pupa, and imago. The splitting of the embryonic life into two stages is to capture the hydropic nature of eggs, i.e., eggs that swell during embryogenesis. The headings from each panel corresponding to each life stage show the level of maturity E_H that controls life-stage transitions, except for the larval stage. The reproduction buffer density, $[E_R]$, controls the onset of pupation and thus the stage transition between larvae and pupa. For the imago, the level of maturity remains constant at $E_H = E_H^e$. The box presented in the pupal stage shows the dynamics of egg production for those species of insects that mature eggs already in the pupal stage. $\dot{p}_{AO}$, $\dot{p}_{GO}$, and $\dot{p}_{RO}$ represent the assimilation, growth, and reproduction overhead fluxes. E_{larv} and E_{R_larv} represent the reserve and reproduction buffer at the onset of pupation. V2 represents the imago new structure that starts to build inside the pupa. See *Materials and methods: A generic DEB model for holometabolous insects* and *Particularities for* Venturia canescens *parasitoids* for further explanations of symbols and implications between stage transitions.

porated for *Venturia canescens* in the embryo and imago stages. These modifications are explained in *Materials and methods: Particularities for* Venturia canescens *parasitoids*.

As in the standard DEB model, the embryo starts mobilizing the maternal reserve for development, growth, and maintenance processes, but it does not assimilate energy from food and it does not allocate energy to reproduction (called embryo1 in Fig. 1). As the individual achieves a particular threshold of energy invested in development, $E_H = E_H^b$, it enters the larval stage. The animal then starts feeding as in the standard DEB model but also starts investing energy to reproduction (larva, Fig. 1). As the stage in which there is allocation to reproduction is called adult stage in DEB terms (see *Materials and Methods: Standard DEB model*), we will use interchangeably the terms imago and wasp instead of adult to refer to the ontogenetic stage that occurs after the parasitoid emerges from the cocoon. A larva starts to fill the reproduction buffer then and continues to allocate energy to maintenance and growth. In DEB theory, allocation to reproduction does not occur as long as maturity is still increasing. We assumed therefore that maturity remains constant at E_H^b during the larval stage. This is a reasonable assumption from a biological point of view as maturity involves cell differentiation. The imaginal discs present in the larvae, which are precursors of imago structures, remain undifferentiated during the larval phase (Chapman et al. 2013). While the reproduction buffer is not yet used to build eggs during the larval stage, the insect accumulates energy that will be needed for building the eggs later, either during the pupal stage or right after the insect emerges from the cocoon, depending on the species (Jervis et al. 2001). The level of nutrient reserves accumulated in the fat body modulates several important aspects of the insect's life, such as the timing of metamorphosis and egg development (Arrese and Soulages 2010). Indeed, recent work shows that energetic thresholds are one of the critical factors affecting the timing of pupation in *Manduca sexta* (Lepidoptera: Sphingidae; Helm 2013). For this, as well as for other species of holometabolous insects, metamorphosis occurs when the larvae achieves a threshold of mass called "critical" (see Suzuki et al. 2013). We assumed therefore that the onset of the pupal stage occurs once the density of the reproduction buffer built during the larval phase achieves a certain threshold $[E_R^j]$. The threshold for pupation is $[E_R^j] = s_j[E_R^m]$, which is introduced with a new parameter s_j and an expression that gives the reference value, i.e., the maximum value for reproduction buffer density, for the onset of pupation

$$[E_R^m] = (1 - \kappa)[E_m] g \frac{\dot{k}_E + \dot{k}_M}{\dot{k}_E - g\dot{k}_M}.$$

(For a detailed explanation of this equation and the associated parameters, see Appendix B.) Therefore, the larval stage is set from $[E_R] = 0$ to $[E_R] = [E_R^j]$. Note that our reproduction buffer density threshold assumption is compatible with the critical mass threshold for pupation hypothesis reported in the literature, as the reproduction buffer contributes to the mass of the animal, and both increase over time.

It is during the time of pupation that the imago structure of the insect is formed, while the larval structures are broken down (Wald 1981, Mane-Padros et al. 2010, Kaneko et al. 2011, Merkey et al. 2011). In the model, this is represented by the conversion of larval structure and reserve to pupal reserve (pupa, Fig. 1). For achieving this, a new parameter is added to the standard DEB model: y_{EV}. Parameter y_{EV} converts larval structure to reserve and its units are in mol/mol. In order to convert it to J/cm^3 of larval structure, we need to specify the chemical potential of reserve (μ_E, J/mol) and the volume-specific mass of structure ($[M_V]$, mol/cm^3) whose values are given in Lika et al. (2011*a*). Moreover, we also need to specify the decay of larval structure in the pupa, $\dot{k}_{E1}$, which relates to energy conductance, so that $\dot{k}_{E1} = \dot{v}/L_j$ where L_j is the structural length of the larva at pupation. Like the embryo, the pupa does not feed and does not allocate energy to reproduction but keeps the reproduction buffer filled during the larval stage, ready to mature eggs. The onset of the pupal stage resets the amount of energy dissipated for maturation to 0, so development is reset at $E_H = 0$ (see Fig. 1, pupa). This reset is needed as maturity is linked to structure and, as we have explained, a new structure is built up from scratch. Since maturation is linked to cell differentiation in DEB theory, and the differentiation of imago structures from the larval imaginal discs starts at the onset of metamorphosis (Arrese and Soulages 2010), it is reasonable to assume that the amount of energy dissipated for maturation is reset at 0 and increases during the pupal phase until imago structures are completely formed. After the completion of the pupal phase, the pupa has achieved a particular threshold of energy invested in development $E_H = E_H^e$, which specifies the timing of emergence of the imago from the cocoon (Fig. 1, pupa).

In some species of insects, egg maturation starts during the pupal stage (Stevens et al. 2000, Jervis et al. 2001, 2005, Jervis and Ferns 2004); therefore, when the individual has achieved a particular threshold of energy invested in development, $E_H = E_H^{eggs}$ it starts maturing eggs from the reproduction buffer. E_H^{eggs} is thus the maturity level at which egg production starts. At this maturity level, the reproduction buffer turnover is specified by a new parameter, $\dot{k}_E$, with units d^{-1}. This introduces a new state variable in the model called egg buffer, E_{eggs}, which is filled by the reproduction buffer (Fig. 1, pupa). Except for the mobilization of the reproduction buffer, the pupa behaves, from an energetic point of view, very much like the embryo. Indeed, after converting larval structure to pupal reserve, it uses this energy supply to fuel maintenance, development, and growth. Once the imago emerges, it

TABLE 4. List of DEB parameters present in the holometabolous insects DEB model and their value for *Venturia canescens* parasitoids.

Parameter	Description	Value	Units
κ_X	assimilation efficiency	0.94	
f	Holling type II scaled functional response	0.95	
$[E_G]$	volume-specific cost of structure	21 210	J/cm^3
$\dot{v}$	energy conductance	0.0207	cm/d
$[\dot{p}_M]$	volume-specific somatic maintenance	245.7	J·d^{-1}·cm^{-3}
κ	fraction of mobilized reserve allocated to soma	0.930	
$\dot{k}_J$	maturity maintenance rate coefficient	0.002	d^{-1}
κ_R	fraction of the reproduction buffer fixed into eggs	0.85	
z	zoom factor	3.98	
δ_M	shape correction coefficient	0.152	
$\ddot{h}_a$	Weibull ageing acceleration	0.004	d^{-2}
s_G	Gompertz stress coefficient	0.0001	
y_{EV}	yield of imago reserve on larval structure	0.8	mol/mol
s_j	threshold for the onset of pupation	0.983	
s_S	threshold for the onset of silk production	0.106	
E_H^x	maturity threshold from embryo1 to embryo2	0.0002	J
E_H^b	maturity threshold from the embryonic stage to the larval stage	0.044	J
E_H^e	maturity threshold at imago emergence	5.56	J
E_H^{eggs}	maturity threshold at egg maturation	5.48	J
$\dot{k}_E$	reserve and reproduction buffer turnover of the imago	0.291	d^{-1}
κ_{SA}	mass coefficient from assimilation to silk production	0.03	
κ_{SG}	mass coefficient from growth to silk production	0.5	
κ_{SD}	mass coefficient from dissipation to silk production	0.94	

starts feeding and stops allocating energy to development and growth. The energy that the imago assimilates is now allocated to somatic and maturity maintenance on one hand, and continues to fill the reproduction buffer to produce the eggs on the other hand (Fig. 1, imago). Indeed, literature shows that there is an influence of food on longevity and reproduction in many species of holometabolous insects (e.g., Glaser 1923, Cheng 1972, Jervis et al. 2008). In this life stage, the reserve and reproduction buffer turnover are both specified by the parameter $\dot{k}_E$. As we mentioned in the introduction, some species of holometabolous insects do not feed after emergence. This is modeled by the absence of assimilation in the imago stage. In these species, the imago fuels its metabolic needs (maintenance and reproduction) by mobilizing energy from the reserve built before emergence (see *Discussion* for further explanation). The energy fluxes, the equations describing the dynamics of the state variables, and the new model parameters for holometabolous insects are shown in Tables 4, 5, and 6, respectively. The maximum surface-area-specific assimilation rate parameter $\{\dot{p}_{Am}\}$ is absent from Table 4. This parameter is internally calculated by the model by using the relationship $\{\dot{p}_{Am}\} = z[\dot{p}_M]/\kappa$ (see Kooijman 2010).

As for the standard DEB model (see *Materials and methods: Standard DEB model*), the variable that more directly controls stage transitions (and hence time and size at maturation) is the level of maturity for all the life stages, except for the larva for which the transition to pupa is controlled by the reproduction buffer density (see Fig.1). The level of maturity controls life-stage transitions from embryo1 to embryo2 (E_H^x), from embryo2 to larva (E_H^b), and from pupa to imago E_H^e.

TABLE 5. Energy fluxes associated to different metabolic processes modeled for a holometabolous insect.

Metabolic process	Energy flux
Larval stage	
Assimilation	$\dot{p}_A = [\dot{p}_{Am}] f V$
Mobilization	$\dot{p}_C = E\dfrac{[E_G]\dot{k}_E + [\dot{p}_S]}{\kappa[E] + [E_G]}$
Somatic maintenance	$\dot{p}_S = \dot{p}_M = [\dot{p}_M]V$
Growth	$\dot{p}_G = \kappa\dot{p}_C - \dot{p}_S = \kappa\dot{p}_C - \dot{p}_M$
Maturity maintenance	$\dot{p}_J = \dot{k}_J E_H^b$
Reproduction	$\dot{p}_R = (1-\kappa)\dot{p}_C - \dot{p}_J$
Pupal stage	
Transformation of larval structure	$\dot{p}_L = V\dot{k}_{El}$
Mobilization of E	$\dot{p}_C = E\dfrac{[E_G]\dot{v}_j/V2^{1/3} + [\dot{p}_S]}{\kappa[E] + [E_G]}$
Somatic maintenance	$\dot{p}_S = \dot{p}_M = [\dot{p}_M]V2$
Growth	$\dot{p}_G = \kappa\dot{p}_C - \dot{p}_S = \kappa\dot{p}_C - \dot{p}_M$
Maturity maintenance	$\dot{p}_J = \dot{k}_J E_H$
Maturation	$\dot{p}_R = (1-\kappa)\dot{p}_C - \dot{p}_J$
Mobilization of E_R	$\dot{p}_{C2} = \dot{k}_E E_R$
Reproduction overhead	$\dot{p}_{RO} = (1-\kappa_R)\dot{p}_{C2}$
Egg flux	$\dot{p}_{R2} = \dot{p}_{C2} - \dot{p}_{RO}$
Imago stage	
Assimilation	$\dot{p}_A = \dot{p}_S + \dot{p}_J$
Mobilization of E	$\dot{p}_C = \dot{k}_E E$
Somatic maintenance	$\dot{p}_S = \dot{p}_M = [\dot{p}_M]V2$
Maturity maintenance	$\dot{p}_J = \dot{k}_J E_H^e$
Reproduction	$\dot{p}_R = \dot{p}_C - \dot{p}_S - \dot{p}_J$
Mobilization of E_R	$\dot{p}_{C2} = \dot{k}_E E_R$
Reproduction overhead	$\dot{p}_{RO} = (1-\kappa_R)\dot{p}_{C2}$
Egg flux	$\dot{p}_{R2} = \dot{p}_{C2} - \dot{p}_{RO}$

Notes: The energy fluxes for the embryo stage are the same as those described for the standard DEB model excluding assimilation and reproduction (see Table 1). In the pupal stage, V refers to larval structure.

Table 6. Equations describing the dynamics of the state variables for the larva, pupa, and imago stages in holometabolous insects.

State variable	Equation
Larval stage	
Reserve (E)	$\frac{dE}{dt} = \dot{p}_A - \dot{p}_C$
Structure (V)	$\frac{dV}{dt} = \frac{\dot{p}_G}{[E_G]}$
Reproduction buffer (E_R)	$\frac{dE_R}{dt} = \dot{p}_R$
Silk (S)	$\frac{dS}{dt} = \kappa_{SA}\dot{p}_A + \kappa_{SG}\dot{p}_G + \kappa_{SD}\dot{p}_D$
Pupal stage	
Reserve (E)	$\frac{dE}{dt} = \dot{p}_L y_{EV}\mu_E[M_V] - \dot{p}_C$
Structure larva (V)	$\frac{dV}{dt} = -\dot{p}_L$
Structure imago ($V2$)	$\frac{dV2}{dt} = \frac{\dot{p}_G}{[E_G]}$
Maturation (E_H)	$\frac{dE_H}{dt} = \dot{p}_R$
Reproduction buffer (E_R)	$\frac{dE_R}{dt} = -\dot{p}_{C2}$
Egg buffer (E_{egg})	$\frac{dE_{egg}}{dt} = \dot{p}_{R2}$
Imago stage	
Reserve (E)	$\frac{dE}{dt} = \dot{p}_A - \dot{p}_C$
Reproduction buffer (E_R)	$\frac{dE_R}{dt} = \dot{p}_R - \dot{p}_{C2}$
Egg buffer (E_{egg})	$\frac{dE_{egg}}{dt} = \dot{p}_{R2}$

Note: The equations describing the dynamics of the state variables at the embryonic stage are the same as those described in the standard DEB model (see Tables 1 and 2).

The reproduction buffer density,$[E_R]$, controls the onset of pupation and thus the stage transition between larvae and pupa at $[E_R^j] = s_j[E_R^m]$. For the imago, the level of maturity remains constant at $E_H = E_H^e$. Therefore, what controls the life-stage transitions are the different maturity and s_j parameters that are estimated through the fitting procedure (see Table 4).

Metabolic acceleration.—An important difference between the standard DEB model and the model for holometabolous insects is that the standard DEB model is built under the assumption that animals do not change shape during their lifespan, i.e., they present an isomorphic growth (Kooijman 2010). Change in shape is crucial in DEB, since feeding is linked to surface area and maintenance is linked to volume (see assimilation and somatic maintenance fluxes in Table 1). The standard DEB model assumes, therefore, that feeding is proportional to surface area and surface area is proportional to volume to 2/3 the power during the whole life of the animal. However, in the case of holometabolous insects this assumption does not hold, since animals change morphology during their lives. Usually these animals present larval stages that have a very different morphology compared to other stages of their lives; they are called V1-morphs, according to Kooijman (2010). These organisms change shape during growth such that the surface area is proportional to volume. Some parameters of the standard DEB model depend on the surface-area–volume relationships: maximum surface-area-specific searching rate $\{\dot{F}_m\}$, maximum surface-area-specific assimilation rate $\{\dot{p}_{Am}\}$, and energy conductance $\dot{v}$. Therefore, the change in shape alters the surface area to volume ratio for the different stages, also influencing the parameters $\{\dot{F}_m\}$, $\{\dot{p}_{Am}\}$, and $\dot{v}$ (note that the dimension of $\dot{v}$ is length/time, but this length is actually a ratio of volume and surface area). For the sake of explanation, we will use Θ to stand for any of the parameters that will be affected by the change from isomorph to V1-morph ($\{\dot{F}_m\}$, $\{\dot{p}_{Am}\}$, and $\dot{v}$). We call metabolic acceleration the process in which a specific stage of an animal's ontogeny behaves as a V1-morph and can be modeled by a change in the parameters Θ (Kooijman 2010). In the present model, we assume that the embryo behaves as an isomorph, the larva as a V1-morph, and after pupation the animal switches back to isomorphy. In the embryo stage, the dynamics of the state variables are ruled by the parameters Θ. During the larval growth, the parameters Θ increase proportional to length, that is, each parameter Θ is replaced by $\Theta L/L_b$, ensuring that the state variables have V1-morph dynamics. L_b is the length at birth, when the larva starts feeding. When the organism eventually reaches pupation, the parameters Θ become once again constant and the dynamics become isomorphic again. The parameters Θ retain the value reached at the end of the larval phase, $\Theta_j = \Theta L_j/L_b$, where L_j is the length at the onset of pupation. We define new parameters to make the dynamics equations explicit in terms of the associated morphity. For the larva, the reserve turnover, $\dot{k}_E$, relates to the energy conductance of the embryo, $\dot{v}$, so that $\dot{k}_E = \dot{v}/L_b$. Similarly, the maximum surface-area-specific searching and assimilation rates are $[\dot{F}_m] = \{\dot{F}_m\}/L_b$ and $[\dot{p}_{Am}] = \{\dot{p}_{Am}\}/L_b$, respectively (see in Table 5, the fluxes making use of these parameters). Notice that the definition of these parameters does not add any degrees of freedom to the model, as they are completely defined by the main parameters presented in Table 4.

Particularities for Venturia canescens *parasitoids*

We have modeled the life history of *V. canescens* parasitoids by using the previously explained generic DEB model for holometabolous insects (Fig. 1). In addition to the modifications concerning holometabolous insects, *V. canescens* shows some further particularities during the embryo, larval, and imago stages that have also been incorporated in the model.

Energy fluxes at the embryonic stage.—*Venturia canescens* is known for having hydropic eggs, which are capable of absorbing hemolymph from their host already at the embryo stage, i.e., the eggs swell during embryogenesis (Fisher 1971, Ohbayashi et al. 1994). This is included in the model by incorporating a new

parameter E_H^x that represents the maturity at the time at which the embryo starts assimilating food from the hemolymph of the host (Table 4). Thus, the embryo stage is subdivided in two stages (see Fig. 1, embryo1 and embryo2). The first embryo stage goes from $E_H = 0$ to E_H^x and is represented by the fluxes and equations of the embryonic stage from the standard DEB model. The second embryonic stage goes from E_H^x to E_H^b, when the larva emerges. In this stage, the organism behaves as the juvenile stage of the standard DEB model: it starts assimilating energy from food and allocates the energy to development, growth, and maintenance (see Table 1).

Silk production during the larval stage.—Some parasitoid species pupate within protective cocoons of silk produced by the larvae themselves (Godfray 1994). In some species that go through three larval instars, silk production starts during the late second instar once the silk glands are well developed (de Eguileor et al. 2001). *Venturia canescens* goes through five larval instars, and we do not know when it starts producing silk. We have assumed that silk production starts when the density of the reproduction buffer built during the larval phase achieves a certain threshold $[E_R^S]$. This is introduced with a new parameter $s_S = [E_R^S]/[E_R^m]$. Silk production starts therefore when $[E_R^S] = s_S[E_R^m]$ (see Appendix B for a full explanation of the expression $[E_R^m]$). For the inclusion of the silk, we have incorporated a new state variable, S(J), that represents the silk produced by the larvae. Silk is considered a product in DEB and changes through time as a linear combination of assimilation, dissipation, and growth (Table 6). To fully specify the change in silk production through time, we have incorporated three new parameters: κ_{SA}, κ_{SG}, and κ_{SD}. These parameters determine the contribution of assimilation, growth, and dissipation flux to silk production, respectively (Table 4).

Energy fluxes at the imago stage.—We made several assumptions to determine the energy fluxes linked to the different processes during the imago stage. Reproduction data on *Venturia canescens* parasitoids shows that they lay eggs until approximately day 17 after emergence and stop laying eggs but continue living until approximately day 36 (see Fig. 2C in Harvey et al. [2001]). These data show that wasps can live much longer after laying all the eggs, which suggests that they emerge with a certain amount of energy in the reserves that will be used to produce eggs. After this energy is depleted, they do not produce more eggs but continue to be alive. We have incorporated this in the model by assuming that the assimilation flux equals the maintenance flux, $\dot{p}_A = \dot{p}_S + \dot{p}_J$, so that wasps ingest as much food as they need to pay maintenance costs and are alive as long as they are ingesting food. We are aware that post-reproductive lifespan of the imago can be a laboratory artifact, but the assumptions that we made on the energy fluxes during the imago stage do not limit the applicability of the model. The lifespan of the organism is completely controlled by the Weibull ageing acceleration parameter $\ddot{h}_a$ (see Table 3). Given that this parameter has no impact in any other model feature, the fitting with a different, more realistic lifespan will only impact the parameter $\ddot{h}_a$, leaving all the other predictions and parameters the same. Indeed, the results did not change after we fitted

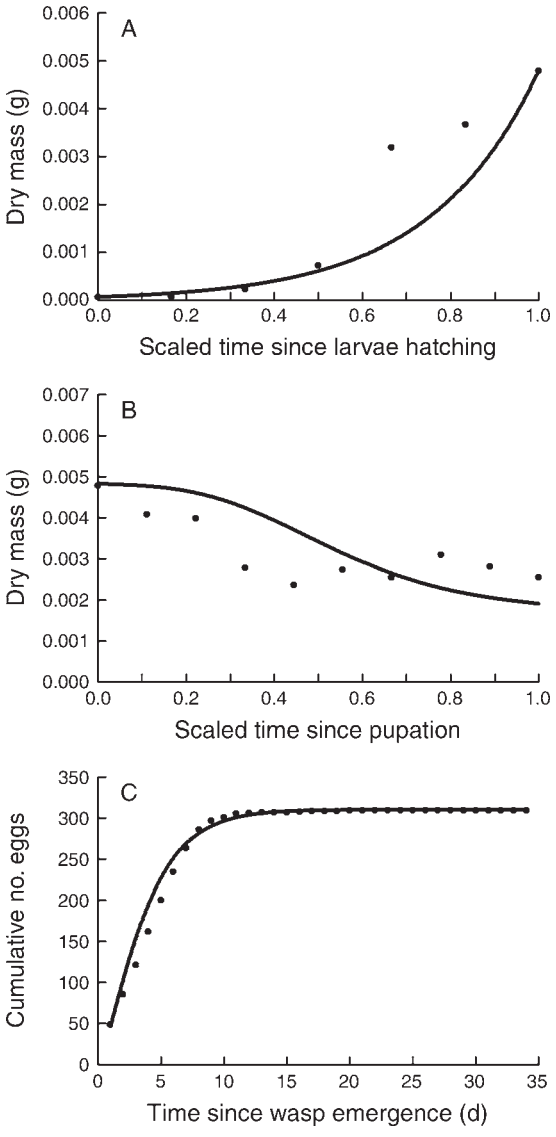

FIG. 2. Fitting of *Venturia canescens* model predictions to observed data. (A) Dry mass of larva since larval hatching, (B) dry mass of pupa since the onset of pupation, and (C) cumulative number of eggs matured after imago emergence through imago lifespan. All predictions were made at an ingestion level, f, set at $f = 0.95$. Observed data were collected from *Venturia canescens* parasitoids parasitizing fifth instars of *Plodia interpunctella*. The line represents the model prediction, and the points represent the observed data collected in Harvey et al. (1994, 2001). Note that, in panels (A) and (B), the time is scaled between 0 and 1, 0 being the start of the larval/pupal phase and 1 being the end of the larval/pupal phase in each subpanel. The scaled value $t = 1$ corresponds to 6 and 5.62 days for the observed and predicted larval developmental times, respectively, and to 9 and 6.43 days for the observed and predicted pupal developmental times, respectively.

TABLE 7. Comparison of the model predictions to observations.

Symbol	Description	Data	Model prediction	Units	Source
a_b	age at larval hatching	4	3.9	d	Harvey et al. (1994)
a_j	age at pupation	10	9.5	d	Harvey et al. (1994)
a_e	age at imago emergence	21.53	16	d	Harvey et al. (1994)
a_m	imago lifespan	36.5	35.88	d	Harvey et al. (1994)
W_{emb}	dry mass of a recently laid egg	1.87×10^{-7}	8.5×10^{-7}	g	Ohbayashi et al. (1994)
W_b	dry mass at larval hatching	6.9×10^{-5}	6.4×10^{-5}	g	Harvey et al. (1994)
W_j	dry mass at pupation	4.77×10^{-3}	4.82×10^{-3}	g	Harvey et al. (1994)
W_e	dry mass at emergence	1.75×10^{-3}	1.00×10^{-3}	g	Harvey et al. (1994)
W_s	mass cocoon shell/mass pupa	0.19	0.18		Howell and Fisher (1977)
N_e	matured eggs at emergence	40.20	48.08	eggs	Harvey et al. (2001)

our model by setting the imago longevity to 17 days, i.e., only the reproductive lifespan (data not shown).

We also know that there is contribution of food to egg production in *V. canescens* wasps (Eliopoulos et al. 2003). This is modeled by a rate of reserve mobilization higher than the influx of assimilated food to fill the reserve, i.e., the output coming out from the reserve is higher than the input, which shows that food is redirected to egg production. The model incorporates a succession of two buffers for egg production. Within the first pool, E, food consumed during the imago stage is mixed with the pool of reserve at imago emergence. The reserve is thus partially filled with nutrients coming from food. The second pool, E_R, initially contains the reproduction buffer at the end of the pupal period. This pool is refilled with a flux coming from the first pool, E, during the imago stage. Finally, egg production is determined by the energy contained in the egg buffer, E_{eggs}, which is refilled with a flux coming from E_R (see Fig. 1, imago). As in the standard model, imagoes convert the reproduction buffer, E_R, to eggs with a constant reproduction efficiency, κ_R. These energy fluxes are described in Table 5 and the resulting dynamics of the reserve, the reproduction buffer, and the egg buffer are shown in Table 6.

Data collection to estimate model parameters

To estimate the DEB model parameters, we used measurements of mass (related to the state variables E, V, and E_R for adult individuals) as a function of time (related to the state variable E_H; Fig. 2). In particular, we focused on published data on the size of a recently laid egg (Ohbayashi et al. 1994), the dry mass through time of the larva and pupa (Harvey et al. 1994), and the number of eggs matured at emergence and after imago emergence (Harvey et al. 2001) of *Venturia canescens* parasitoids parasitizing fifth instars of *Plodia interpunctella* (Lepidoptera: Pyralidae) host. Data reported on egg production were those collected under constant food and host access (Harvey et al. 2001). Data reported in Harvey el al. (2001) show the number of progeny instead of the number of eggs. To calculate the number of eggs from the number of progeny, we used the percentage of survival of *V. canescens* parasitoids at emergence when they develop in *P. interpunctella* hosts at 25°C (see Spanoudis and Andreadis 2012). The survival at emergence is around 83% under these temperature conditions, thus we multiplied the number of progeny by 100/83 to get an estimation of the number of eggs.

The data on the embryo size (length, $l = 0.027$ cm, and width, $w = 0.0047$ cm; Ohbayashi et al. 1994) were used to estimate embryo mass by assuming that the egg has a cylindrical shape and that the density of the egg is $d = 0.4$ g/cm^3.

We also used data related to the specific lifespan events (Table 7), time and mass, at larval hatching, at pupation, and at imago emergence (Harvey et al. 1994). In addition, we used data on the average parasitoid lifespan (Harvey et al. 1994), as well as mass of the cocoon shell divided by the mass of the cocoon to determine the parameters related to silk production (Howell and Fisher 1977). All data were obtained at 25°C.

Parameter estimation

The parameterization procedure has been described in detail in Lika et al. (2011*a*, *b*). The estimation was completed using the downloadable software DEBtool (Kooijman et al. 2008; *available online*)[7] run in MATLAB (Mathworks, Natick, Massachusetts, USA). All parameters were estimated simultaneously using weighted sum of squares routines (nmregr.m) with the Nelder-Mead simplex method, generally followed by a Newton Raphson optimization. The goodness of fit of the parameter estimates was quantified by the mean relative error for the real data, i.e., 10(1 − mean relative error) (Lika et al. 2011*a*, *b*). A mean relative error of 0 gives the highest mark of the goodness of fit, i.e., 10. A copy of the MATLAB model code can be found in Supplements 1 and 2.

Model validation

To validate our model, we used an independent data set to compare the mass change during pupation between real observations reported in Howell and Fisher (1977) and model predictions. We used the dry mass of the larva at the end of the larval period and the dry mass of the wasp at emergence. The data used to validate our model were data on the growth of *Venturia canescens* parasitoids developing in *Ephestia kuehniella* (Lepidop-

[7] http://www.bio.vu.nl/thb/deb/deblab/index_main.html

tera: Pyralidae) host at 25°C. The mass of the hosts used in Howell and Fisher's paper was heavier than the host's mass reported in the paper from which we collected the data to estimate the model parameters, i.e., 10.48 mg vs. 7 mg of host, respectively. Therefore, when comparing real data to model predictions, we ran our model by assuming that *Venturia* ingestion is maximal when it develops in *Ephestia*. The scaled functional response thus attains its maximal value, i.e., $f = 1$. We used the proportional mass loss from pupation to emergence between predicted and observed data to validate our model.

For model validation, we also used published data on the developmental times, from egg to pupation, from pupation to emergence, and from emergence to death of *Venturia canescens* parasitoids developing on fifth instars of *Plodia interpunctella* hosts at different temperatures: 17.5°, 20°, 22.5°, 25°, 27.5°, 30°, and 32.5°C (Spanoudis and Andreadis 2012). We thus ran model simulations at all those temperatures to compare real data and model predictions. Note that for imago longevity, we used the reproductive lifespan and ignored the post-reproductive lifespan, given that the value of imago longevity shown in Spanoudis and Andreadis at 25°C was 17 days.

We also used published data on the cumulative number of progeny two days after wasp emergence under starving conditions at 25°C (Harvey et al. 2001) from wasps that developed in fifth instars of *P. interpunctella* host. To calculate the number of eggs from the number of progeny, we used the percentage of survival of *V. canescens* parasitoids at emergence when they develop in *P. interpunctella* hosts at 25°C (see Spanoudis and Andreadis 2012). Hence, we multiplied the number of progeny by 100/83 to get an estimation of the number of eggs (see *Materials and methods: Parameter estimation*). This data was compared to the cumulated number of eggs predicted by the model two days after eclosion after setting $f = 0$, i.e., with no food ingestion.

Predictions of whole life-cycle energetics

We computed the dynamics of the state variables, E, V, E_H, E_R, and E_{eggs}, for the whole parasitoid life cycle once we got an estimation of the parameters that provided a satisfactory fit of the model predictions to the data. To express all the state variables in Joules, we converted V from cm^3 to Joules by using the chemical potential of structure μ_V (J/mol) and the volume-specific mass of structure $[M_V]$ (mol/cm^3), whose values are given in Lika et al. (2011*a*).

Model simulations: contribution of larval and imago feeding to egg production

Food variation was entered in the model by running simulations with different values of the scaled functional response, f, in the juvenile and imago stages (see Table 4). The dimensionless function f scales ingestion rate in relation to food concentration according to a Holling type II functional response. Note that f is not a parameter but a function of a (possibly varying) food density. At constant food density it can, however, be treated as parameter. The parameter called scaled functional response can reach a value between 0 and 1, where 0 corresponds to no food ingested and 1 to maximal food ingested. For the imago stage, we ran simulations by setting f to 0 and 1. We chose these values of f for the purpose of comparison. A zero f during the imago stage implies that the animal does not assimilate after emergence. In this case, we have a full capital breeder, i.e., a parasitoid that invests only capital resources in egg maturation because it does not feed after emergence. By comparing egg production between a parasitoid that feeds ad libitum ($f = 1$) and a parasitoid that does not feed ($f = 0$) after emergence, we can understand which proportion of egg production is attained from capital and which from income resources.

For the juvenile stages, the embryo and larval stages feed from the hemolymph and tissues of the host. The functional response of *Venturia*'s juvenile stages must be linked to the state variables of the hosts. As the aim of this work is not to model the parasite–host interaction in such detail, we have used different and fixed values of f as a proxy of the quantity of host ingested (i.e., host size). We therefore ran model simulations at different values of ingestion level, from $f = 0.91$ to $f = 1$ during the early stages of development, i.e., embryo and larval stage, to determine the effect of food ingestion early in life on egg production and longevity later on. The maximum value of ingestion $f = 1$ was chosen by assuming that the food availability is maximum when *Venturia* develops in *Ephestia kuehniellia* hosts. We made this assumption because we know from the literature that *Venturia* is able to parasitize and fully consume *E. kuehniellia* final instar hosts and that these hosts are much heavier compared to *P. interpunctella* hosts (Howell and Fisher 1977, Harvey et al. 1994). In addition, the dry mass of a final instar larva attained by *Venturia* is 5.495 mg and that of the imago is 1.9 mg, which is able to lay up to 700 eggs when it develops in a fully grown larva of *E. kuehniellia* host at 25°C (Howell and Fisher 1977, Roberts and Schmidt 2004). We verified that our model showed realistic results after setting $f = 1$ as the maximum: the predicted dry mass of a final instar larva and of an imago were 5.1 mg and 1.3 mg, respectively, and the predicted total amount of eggs laid were 711 eggs. The ingestion range between $f = 0.91$ and $f = 1$ is equivalent to 6.23 mg and 7 mg of host ingested, respectively. The amount of host ingested during the parasitoid development was estimated from the total joules ingested at the end of the larval period at the different values of ingestion level. At each ingestion level, the conversion of joules ingested at the end of the larval period into milligrams was done by assuming that each mg of host contains 18.84 J. The last conversion

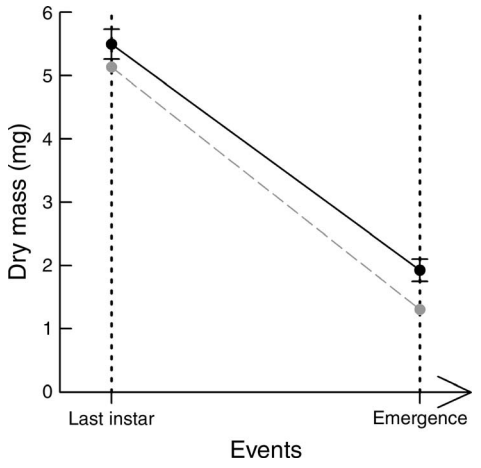

FIG. 3. Comparison between observed (black points) and predicted (gray points) dry mass of *V. cancescens*. The points represent the mass of the larva at the end of the larval period and the mass of the imago at emergence. Predictions were made at an ingestion level set at $f = 1$, i.e., assuming that the parasitoid develops on *Ephestia* host (see *Materials and Methods: Model validation* for further explanation). Error bars represent standard errors. Observed data are reported in Howell and Fisher (1977).

was estimated by using the total mass of host consumed at the end of the larval period for parasitoids developing at fifth instars reported in Harvey et al. (1994), i.e., 6.5 mg of host, and the predicted amount of energy ingested by the parasitoid at the end of the larval period, i.e., 122.4527 J. The lowest value of ingestion level was set at $f = 0.91$ because the model did not show realistic results for ingestion levels below 6.23 mg (see *Discussion* for further explanation).

RESULTS

Model fit

The goodness of fit of the observed to predicted data was 8.9/10 (Lika et al. 2011*a*, *b*). Overall, the model predicted the larval and pupal growth curves well (Fig. 2A, B). The predicted cumulative number of eggs produced during the imago stage was also close to the real data (Fig. 2C). In addition, the comparison between the specific lifespan events collected from the literature and the model predictions also showed a satisfactory similarity (Table 7). The worst prediction was the mass of a recently laid egg, i.e., mass of the embryo (see Table 7). Moreover, the prediction of the time at emergence was underestimated by the model: while wasps emerged approximately on day 21 after oviposition, the model predicted wasp emergence on day 16. This was due to the difference between the observed and predicted duration of the pupal phase, 11 vs. 6.5 days, respectively.

Result of model validation

The comparison between the dynamics of the mass change during pupation showed a similar pattern between observed and predicted data (Fig. 3). Overall, the proportion of mass loss from pupation to emergence was similar between observed and predicted data at 65% and 74% of mass loss, respectively.

The comparisons of the different developmental times between model predictions and observations show that our model captures the qualitative pattern of the thermal response in the data well (see Fig. 4). Both model predictions (solid circles) and real observations (open circles) show that an increase in temperature reduces the different developmental times (see Fig. 4). The predicted developmental times show lower values compared to real data for the embryonic-larval (Fig. 4A) and pupal (Fig. 4B) stages and very similar values for the imago lifespan (Fig. 4C). The quantitative differences between the model predictions and observations in the embryonic-larval and pupal developmental times can potentially be explained by the different feeding conditions of the hosts used in the different studies. Our model was developed using the data collected by Harvey et al. (1994). In Harvey's study, the hosts were fed with a mix of wheat middlings, yeast, and glycerol

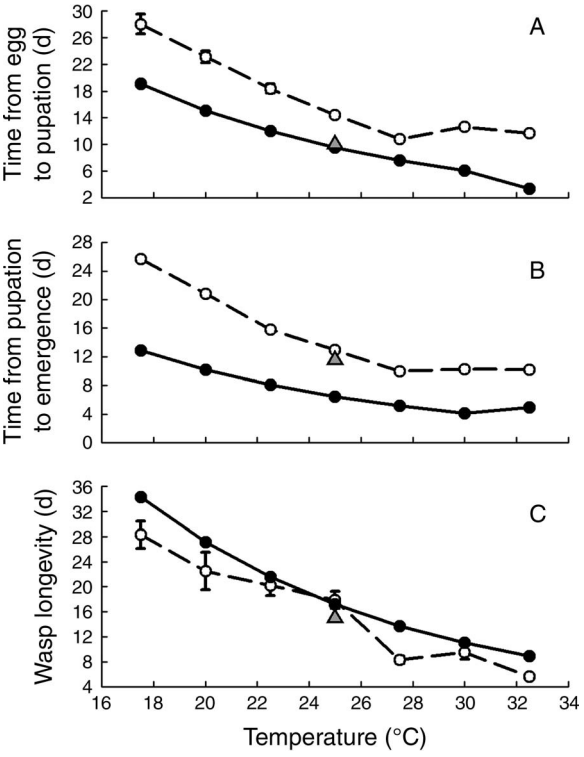

FIG. 4. Comparison between observed (open circles) and predicted (filled circles) developmental times of *Venturia canescens* parasitoids developing at different temperatures in fifth instars of *Plodia interpunctella* host. The different subpanels show the developmental times (A) from egg to pupation, (B) from pupation to emergence, and (C) from emergence to death. Error bars represent standard errors. Empty circles represent the observed data reported in Spanoudis and Andreadis (2012). Gray triangles represent the observed data reported in Harvey et al. (1994) and used to estimate the parameters of the model.

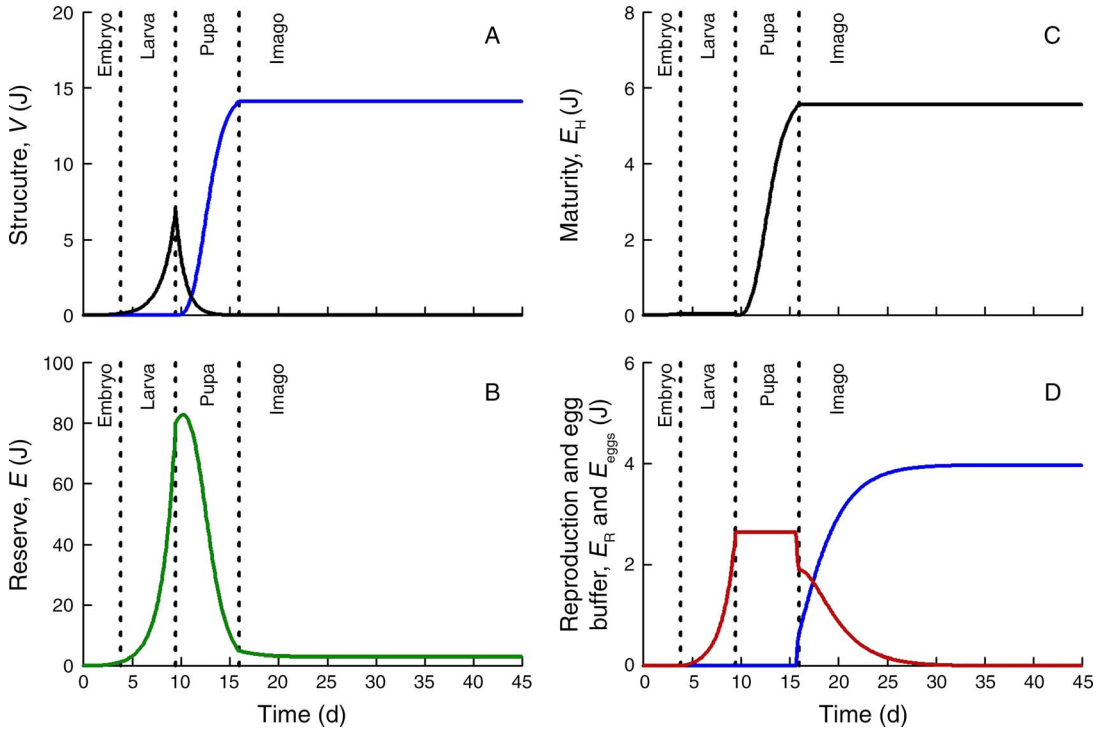

FIG. 5. Dynamics of the DEB state variables from for *Venturia canescens* parasitoids. The dashed lines represent the duration of the embryo, larval, pupa, and imago stage. In panel (A), the black line represents the dynamics of the structure of the embryo and the larvae; the blue line represents the dynamics of the imago structure. In panel (D), the red line represents the dynamics of the reproduction buffer; the blue line represents the joules stored in the egg buffer. The sudden dip in the reproduction buffer before imago eclosion is due to the production of eggs, which drains the reproduction buffer during the pupal stage. The reproduction buffer is replenished once the imago starts feeding but continue to decrease because the input (energy coming from the reserve) is lower than the output (energy taken from the reproduction buffer to mature eggs).

(10:1:1), and the authors gave 25 g of food to 200 *Plodia* eggs. It has been reported elsewhere that Harvey et al. (1994) reared hosts with an excess of food (Jervis 2005). In the study used for model validation (Spanoudis and Andreadis 2012), the hosts were fed with an artificial diet modified by the addition of 450 g dry pinto beans and 31 g agar (they do not mention the number of larvae that were fed with this amount of food). It is therefore likely that the fifth instar larvae of *Plodia interpunctella* hosts used by *Venturia* in both studies achieved different sizes. We know from the literature that host size affects the larval and pupal developmental time, as developmental time from egg to wasp emergence decreases with host size at oviposition (Harvey and Strand 2002).

The cumulative number of eggs two days after emergence at 25°C under starving conditions predicted by the model was very similar to that reported in the literature: 100 vs. 87 ± 11 eggs, respectively.

Predictions of whole life-cycle energetic

The structure formation starts at the beginning of the embryo stage, reaching 0.00078 J and 0.1173 J at the end of the first and second embryo stage, respectively (Fig. 5A). Structure formation continues during the larval stage, reaching a maximum at 6.95 J at the end of the larval stage. During pupation the larval structure disappears and its energy is used, together with energy from the reserve buffer, to build the imago structure. At wasp emergence the imago structure stores 14.11 J and remains constant until the end of the parasitoid life.

Maturity increases from 0 to 0.00029 J during the first embryo stage, it continues up to 0.045 J during the second embryo stage, and remains constant during the larval stage. After pupation maturity restarts from 0, and it reaches 5.56 J at wasp emergence. After wasp emergence, maturity remains constant (Fig. 5C).

Most of the reserve is built during the larval stage and used after pupation (Fig. 5B). Although not visible in the figure due to the chosen scale, there is no increase in the reserve by feeding in the first embryo stage: the reserve changes from 0.013 J at time 0 to 0.009 J at time 0.48 days, the timing at which the second embryo stage starts, equivalent to maturity level $E_H^x = 0.00029$ J. It is not until the onset of the second embryo stage that the parasitoid starts refilling the reserve buffer by feeding. At the end of the embryo stage, the reserve increased up to 1.35 J. During the larval stage, the accumulation of reserve continues until it reaches a maximum (i.e., 80.14 J) at the end of the larval period. At the end of pupation, the

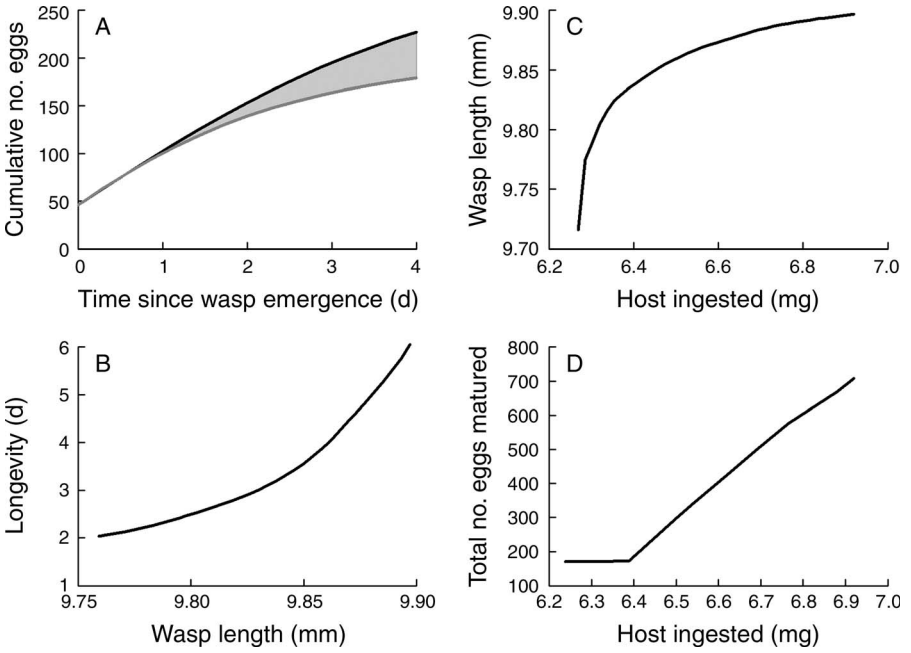

FIG. 6. Effect of capital and income reserves on *Venturia canescens* parasitoid's fitness and life history traits. Panel (A) shows the predicted number of eggs matured after imago emergence for feeding (straight line) and starving (gray line) females until day 4 after imago emergence, the time of death under starving conditions. The ingesta during the embryo and larval stages is $f = 0.95$. The gray area between the black and the gray line corresponds to the cumulated number of eggs that result from the incorporation of income resources through feeding. Panel (C) shows the relationship between the total amount of food ingested at the end of the larval period and the size of the wasp. Panel (B) shows the relationship between longevity and size of the wasp under starving conditions, from emergence onward. Longevity is defined as the time at which the maintenance cost to survive one day equals the total amount of energy stored in both the reserve and the reproduction buffer. Panel (D) shows the total number of eggs matured at the end of the female life as function of amount of food ingested at the end of the larval period.

parasitoid has 4.91 J in the reserve, and it is thus during metamorphosis that the parasitoid uses most of the accumulated reserve. After wasp emergence, the parasitoid continues to use the stored reserve until the reserve buffer reaches a level of 2.89 J and remains constant until the end of the parasitoid's life.

The reproduction buffer starts appearing at the onset of the larval phase and grows until it accumulates a total of 2.64 J (Fig. 5D). During pupation, the reproduction buffer remains constant until the parasitoid reaches a certain maturity threshold, $E_H^{eggs} = 5.48$ J, at which egg maturation starts. From E_H^{eggs} until E_H^e (which is the maturity at wasp emergence) the wasp matures eggs from the reproduction buffer. The reproduction buffer is therefore emptied from 2.64 J to 1.89 J during this period, which translates into a total of 48.08 eggs matured at wasp emergence, equivalent to 0.63 J stored in the egg buffer. After emergence, the imago continues to produce eggs. The wasp produces a total of 300 eggs at the end of its life, equivalent to 3.97 J of accumulated energy in eggs. From emergence until death, the reproduction buffer decreases from 1.89 J until it is emptied approximately on day 34. During this period, the input (energy coming from the reserve) is lower than the output (energy taken from the reproduction buffer to mature eggs) and thus the reproduction buffer decreases.

Results of model simulations

The model simulations show that the food ingested during the imago stage greatly affected egg production. Wasps simulated to feed ad libitum produce a higher number of eggs compared to those simulated not to feed after emergence (Fig. 6A). In addition, feeding conditions experienced during the juvenile stages greatly affected imago performance: the amount of host ingested early in life positively affected wasp length at emergence (Fig. 6C). There was also a positive relationship between wasp length and wasp longevity under food deprivation conditions after emergence (Fig. 6B), and the amount of host ingested early in life positively affected the total number of eggs matured at the end of the parasitoid's life (Fig. 6D).

DISCUSSION

We start the discussion by explaining what we have learned with our model and by describing the implications of our model for *Venturia canescens* and other parasitoid species. We continue by explaining potential reasons for the differences between model predictions and observations. We conclude our discussion with implications regarding life-history traits, host–parasite population dynamics, and climate-change responses in holometabolous insects.

Impact of wasp feeding

The holometabolous DEB model enables us to distinguish and follow the energy invested in an egg through capital or income investment in *V. canescens* (Fig. 6A). The model predicts that females produce fewer eggs when they do not feed after emergence compared to when they do, with the difference being noticeable one day after wasp emergence (Fig. 6A). This is because wasps start maturing eggs from the energy stored in the reproduction buffer during the larval stage; it is not until the second day after emergence that one can notice that the reproduction buffer is being refilled by the food ingested that flows from the reserve to the reproduction buffer. One of the assumptions underlying the construction of the DEB model is that the wasp eats as much as it needs to cover the maintenance costs of living. When feeding, wasps therefore mobilize the reserve with which they emerge to produce eggs and pay the maintenance costs. In contrast, when wasps do not feed, they need to pay maintenance from the reserve buffer, leaving less reserve energy for egg production. In the long term, the impact of imago feeding on egg production is even more striking as feeding wasps produce almost twice as many eggs as nonfeeding wasps (300 vs. 176 eggs), given that feeding wasps also live longer.

Impact of larval feeding: carryover effects over ontogeny

The conditions experienced early in life may have strong effects on the phenotype of the adult, affecting in turn the fitness of the animal. For example, when nutritional conditions during the juvenile stage are good, adults tend to have a larger body size (Day and Rowe 2002), a trait that is strongly correlated with fitness in a wide range of species (Rowe and Ludwig 1991, Honek 1993, Abrams and Rowe 1996, Nylin and Gotthard 1998). In parasitoids, Rivero and West (2002) studied the physiological costs of being small in *Nasonia vitripennis* (Hymenoptera: Pteromalidae). They showed that the number of mature eggs in small wasps is greatly affected by the feeding conditions that they experience after emergence due to the carryover effects over ontogeny. Smaller wasps emerge with lower amount of lipids and glycogen in the reserve. If they do not feed, they mature fewer eggs than when they do feed because presumably they do not refill the energy buffer for eggs. The environment does not alter egg maturation so dramatically for larger wasps because they can still use the large amount of reserves built during the larval stage for maturing eggs. In addition, their results showed that wasp size affected wasp longevity only in starved females.

The results of our work allow us to expand the conclusions of Rivero and West to the whole life-cycle of a parasitoid species and to both growth and reproduction. With respect to growth, the results of our model show that there is a positive relationship between the amount of food ingested during the early stages of the parasitoid development and the wasp length at emergence. If parasitoids eat more during the embryo and larval stages, they also grow bigger (see Fig. 6C), confirming some results of an earlier study by Harvey et al. (1994). We have run the model for different ingestion levels, ranging from 6.23 to 7 mg across the lifetime. Below the lower ingestion level, parasitoids do not ingest enough food during larval stage to store sufficient energy to survive the pupation period. Female *V. canscens* sometimes oviposit in second instar hosts of *P. interpunctella*, hosts that present a maximum dry mass around 4.90 mg (or approximately 70% of the mass of the host instar fifth, as reported in Harvey et al. [1994]). If they do this, larvae are known to then delay their development, allowing the parasitoid larva to wait until the host grows bigger to ingest more food to complete its development. It is thus possible that the parasitoid larva waits until the host weighs approximately 6.23 mg to complete its development successfully. In addition, given that longevity is linked to size in several parasitoid species (Harvey et al. 1994, Rivero and West 2002), these results also have potential implications on parasitoid survival, as we could expect that larger parasitoids will also live longer. Indeed, similar to the results of Rivero and West (2002), we find that wasp size affected wasp longevity in the absence of food after emergence (see Fig. 6B). This only holds, however, under food deprivation conditions. We cannot extend this result to situations with food, as the model, by construction, assumed that wasps can ingest as much as they need to cover maintenance costs in the presence of food.

With respect to reproduction, the results of our model show that there is a positive relationship between the amount of food ingested during the early stages of the parasitoid development and the number of eggs produced by the imago (Fig. 6D). Below a given threshold, wasps emerge with very little energy in the reserve, and not enough of that energy is mobilized to pay maintenance costs to survive the first day after emergence. Under this scenario, wasps then also use part of the energy stored in the reproduction buffer to live. This is valid only on the first day after emergence. Wasps have enough energy to pay maintenance by the second day, because we assumed that wasps take as much food as they need to cover maintenance costs. Above the threshold, wasps mobilize enough energy from the reserve to cover maintenance costs on the first day after emergence and also to refill the reproduction buffer, and hence, to build more eggs. This explains the change of slope between number of matured eggs and food ingested from the threshold onwards.

To summarize these analyses, our mechanistic model provided a framework for interpreting the underlying processes, i.e., energy fluxes, driving patterns shown in real data for *V. canescens* parasitoids. In particular, the model enabled us to distinguish and follow the energy invested in eggs through capital and income reserves.

The predictions show that feeding wasps produce almost twice as many eggs as nonfeeding wasps by incorporating income resources and living longer. Our results also show that the energy stores with which imagoes emerge are heavily affected by how the energy is stored and used in earlier stages, implying that capital resources also have direct implications in the life-history traits and the fitness of the animal. These results highlight the impact of the energy harvested during earlier stages of the insect's life on imago performance. Although it has been well recognized that the reserves accumulated during the larval stages partly determine the fitness of animals in holometabolous insects (O'Brien et al. 2000, Rivero et al. 2001, Min et al. 2006, Wessels et al. 2010), most of the research on insect energy budgets focuses on the energy dynamics during the imago stage (Rivero and West 2002, Casas et al. 2005, Aluja et al. 2011). As far as we know, our study is unique in providing a complete dynamic energy budget in holometabolous insects, by incorporating all the life stages from embryo to imago. We found that most of the reserve built during the larval stage is used during the pupal stage. The final larval instar harvests around 61 times the energy of a recently hatched larva. Around 90% of this energy is then used during pupation. Imagoes therefore emerge with only a small percentage, around 10%, of the maximal energy stored by the larvae (Fig. 5B). While the exact numbers shown in the figure are specific to *V. canescens*, the overall dynamics are likely true for most holometabolous insects. Indeed for other parasitoid species, such as *Aphidius ervi* (Hymenoptera: Braconidae), the imago mass is also correlated with the maximum mass attained by the larva (Sequeira and Mackauer 1992).

Differences between model predictions and observations

The model predicted an embryo's mass to be 4.5 times heavier compared to the mass estimated from real data (see Table 7). While the whole data set used to estimate the parameters of the model was collected under the scenario of the parasitoid developing in *P. interpunctella* hosts, the data used for the embryo mass were form individuals developing in *Ephestia kuehniella* hosts. This may explain the difference between the model predictions and observations for the mass of the embryo. In addition, the food type of the wasps from which we obtained data of recently laid embryos vs. data on egg production through time differed, i.e., sugar vs. honey, respectively. Given that imago feeding affects egg production in *V. canescens*, the different feeding conditions may have also affected egg size and thus mass. In addition, the model predictions show an exponential increase of larval growth during the whole larval stage, while the data show a different pattern from an exponential increase in mass at the end of the larval phase (for the last three points the growth increase is not exponential; see Fig. 2). The inclusion of the wandering phase within the larval phase could improve the fitting of the model to the real growth trajectories of the larva. During the wandering phase, the larva stops feeding, hence, prior to the wandering phase, the larva presumably decreases its ingestion rate until it completely stops feeding before entering pupation. This could explain the patterns of growth trajectories shown by the data and not being captured by the model. For the pupa, we do not have a good argument to explain the differences in mass trajectories between observations and predictions (see Fig. 2). The pupa actually gains some mass from the fourth data point shown in the graph onward. The fact that the pupa gains mass is against mass conservation laws as mass gain should not occur if the animal does not consume resources (especially when we talk about dry mass, as variations in water content could explain the alterations in wet mass). The mass increase through time in the pupa may thus be an experimental artifact.

Implications

The formulation of the DEB model for holometabolous insects, in general, and for *Venturia canescens*, in particular, provides new opportunities to address questions spanning from life-history strategies and climate-change responses in insects to food-web structure and population dynamics of host–parasitoid systems. We highlight these developments only cursorily, as some of them will be the focus of dedicated publications.

Our model can be applied to species that differ in life-history strategies, with strategies ranging from income breeding to capital breeding (Stearns 1992, Tammaru and Haukioja 1996, Jonsson 1997, Casas et al. 2005, Jervis et al. 2007, 2008, Stephens et al. 2009). The choice of breeding strategy can be made by choosing an assimilation rule for the imago stage. The model can be applied to capital breeders that do not feed during the imago stage by setting the assimilation flux during this stage to 0. In this case, the investment in egg production can only come from what has been accumulated in the reserves in the previous life stages. For other types of capital breeders that feed during the imago stage but for which there is not contribution of feeding to egg production, the assimilation can be chosen so that the mobilization flux will approximate the maintenance flux. For these species, the mobilized energy pays exclusively the maintenance costs, and there will be no surplus of the mobilized energy invested in reproduction. For a mixed-capital and income-breeding strategy, we can use the same model that we used for *Venturia* with a higher assimilation flux. These species feed during the imago stage, and there is contribution of feeding to egg production: the surplus of energy mobilized that is not used to pay maintenance is invested in reproduction. For income breeders, i.e., species that feed during the imago stage for which there is always contribution of feeding to egg production, the model can be the same. Having different values for the model parameters would,

however, allow us to use a lower ratio between the energy stored in the reserve at imago emergence used for reproduction and the accumulated assimilation flux throughout the imago stage used for reproduction. Thus, the model can be used to compare species that present different life-history strategies. We could, for example, study the consequences of larval vs. imago nutrition on reproductive traits for species that present different breeding strategies, thereby obtaining insights about the adaptive value of each strategy. The comparisons between insect species can also be done on the basis of DEB parameters values as it has been done in fish, for example (Lika et al. 2014). In addition, given applicability of DEB theory to all animal species, the holometabolous insects can not only be compared to other insects species on the basis of the parameter values, but also to noninsect species, which will help to discover evolutionary adaptations and patterns (Kooijman 2013, Lika et al. 2014).

While our model assumes a constant environment, real organisms experience fluctuating environments. The DEB formulation can readily be extended to incorporate the consequences of environmental variability (Kearney et al. 2010*a*, 2013, Kearney 2012). The temperature dependence of biological rates can be integrated into the model by ensuring that the DEB parameters with time dimensions scale appropriately with temperature. This is commonly achieved by using the Boltzmann-Arrhenius temperature correction factor (Gillooly et al. 2001, Kooijman 2010). A complete model of the lifecycle bioenergetics of the Australian butterfly *Heteronympha merope* is currently being developed to understand how its distribution and phenology in Australia is expected to change under future climates (Kearney et al. 2010*b*, Barton et al. 2014). A mechanistic model of the butterfly's lifecycle bionenergetics will result in a species distribution model that is more strongly grounded in the underlying ecophysiological processes driving species abundance. DEB models can also readily incorporate the effects of variable food availability (Pecquerie et al. 2009). In the case of *Venturia canescens*, our model is valid for a range of host sizes. Host size has many impacts on the life history traits of parasitic wasps (Godfray 1994, Vet et al. 1994).

The capacity to develop whole life-cycle models of energetics for holometabolous insects given by our DEB model provides new opportunities to study multitrophic interactions and food webs. One promising avenue of application is in physiologically structured population dynamics modeling (Gordon et al. 1991). The extensive knowledge of *Venturia* bioenergetics in the lab and in the field (e.g., Howell and Fisher 1977, Casas et al. 2003, Amat et al. 2012), as well as its use as one of the classical systems of host–parasitoid interactions from the 1960s onward (Takahashi 1959, White and Huffaker 1969), makes this parasitoid species one of the very few for which this task is feasible.

Acknowledgments

We thank E. Desouhant and P. Pelosse for providing us data on *Venturia*'s eggs, and two anonymous reviewers for their helpful comments in a previous version of the manuscript. This work was funded by a Fondation de France post-doctoral fellowship to A. L. Landres and J. Casas. It was also partly funded by the Agroeco project of the Region Centre to J. Casas, and by the CNRS and a grant to J. Maino from the National Science Centre, Poland within HARMONIA (2012/06/M/NZ/00137).

Literature Cited

Abrams, P. A., and L. Rowe. 1996. The effects of predation on the age and size of maturity of prey. Evolution 50:1052–1061.

Aluja, M., A. Birke, L. Guillen, F. Diaz-Fleischer, and D. Nestel. 2011. Coping with an unpredicand stressful environment: the life history and metabolic response to variable food and host availability in a polyphagous tephritid fly. Journal of Insect Physiology 57:1592–1601.

Amat, I., S. Besnard, V. Foray, P. Pelosse, C. Bernstein, and E. Desouhant. 2012. Fuelling flight in a parasitic wasp: which energetic substrate to use? Ecological Entomology 37:480–489.

Applebaum, S. L., T. C. F. Pan, D. Hedgecock, and D. T. Manahan. 2014. Separating the nature and nurture of the allocation of energy in response to global change. Integrative and Comparative Biology 54:284–295.

Arrese, E. L., and J. L. Soulages. 2010. Insect fat body: energy, metabolism, and regulation. Annual Review of Entomology 55:207–225.

Barrett, E. L. B., J. Hunt, A. J. Moore, and P. J. Moore. 2009. Separate and combined effects of nutrition during juvenile and sexual development on female life-history trajectories: the thrifty phenotype in a cockroach. Proceedings of the Royal Society B 276:3257–3264.

Barton, M., P. Sunnucks, M. Norgate, N. Murray, and M. Kearney. 2014. Co-gradient variation in growth rate and development time of a broadly distributed butterfly. PLoS ONE 9(4):e95258.

Brown, J. H., J. F. Gillooly, A. P. Allen, V. M. Savage, and G. B. West. 2004. Toward a metabolic theory of ecology. Ecology 85:1771–1789.

Casas, J., G. Driessen, N. Mandon, S. Wielaard, E. Desouhant, J. Van Alphen, L. Lapchin, A. Rivero, J. P. Christides, and C. Bernstein. 2003. Energy dynamics in a parasitoid foraging in the wild. Journal of Animal Ecology 72:691–697.

Casas, J., S. Pincebourde, N. Mandon, F. Vannier, R. Poujol, and D. Giron. 2005. Lifetime nutrient dynamics reveal simultaneous capital and income breeding in a parasitoid. Ecology 86:545–554.

Chapman, R. F., S. J. Simpson, and A. E. Douglas. 2013. The insects: structure and function. Fourth edition. Cambridge University Press, Cambridge, UK.

Cheng, H. H. 1972. Oviposition and longevity of the dark-sided cutworm, *Euxoa messoria* (Lepidoptera: Noctuidae), in laboratory. Canadian Entomologist 104:919–925.

Cover, M. R., and V. H. Resh. 2008. Global diversity of dobsonflies, fishflies, and alderflies (Megaloptera: Insecta) and spongillaflies, nevrorthids, and osmylids (Neuroptera: Insecta) in freshwater. Hydrobiologia 595:409–417.

Day, T., and L. Rowe. 2002. Developmental thresholds and the evolution of reaction norms for age and size at life-history transitions. American Naturalist 159:338–350.

de Eguileor, M., A. Grimaldi, G. Tettamanti, R. Valvassori, M. G. Leonardi, B. Giordana, E. Tremblay, M. C. Digilio, and F. Pennacchio. 2001. Larval anatomy and structure of absorbing epithelia in the aphid parasitoid *Aphidius ervi Haliday* (Hymenoptera, Braconidae). Arthropod Structure and Development 30:27–37.

Eliopoulos, P. A., J. A. Harvey, C. G. Athanassiou, and G. J. Stathas. 2003. Effect of biotic and abiotic factors on reproductive parameters of the synovigenic endoparasitoid *Venturia canescens*. Physiological Entomology 28:268–275.

Elser, J. J., R. W. Sterner, E. Gorokhova, W. F. Fagan, T. A. Markow, J. B. Cotner, J. F. Harrison, S. E. Hobbie, G. M. Odell, and L. J. Weider. 2000. Biological stoichiometry from genes to ecosystems. Ecology Letters 3:540–550.

Fisher, R. C. 1971. Aspects of the physiology of endoparasitic hymenoptera. Biological Reviews 46:243–278.

Getz, W. M. 2011. Biomass transformation webs provide a unified approach to consumer-resource modelling. Ecology Letters 14:113–124.

Gillooly, J. F., J. H. Brown, G. B. West, V. M. Savage, and E. L. Charnov. 2001. Effects of size and temperature on metabolic rate. Science 293:2248–2251.

Glaser, R. W. 1923. The effect of food on longevity and reproduction in flies. Journal of Experimental Zoology 38:383–412.

Godfray, H. C. J., editor. 1994. Parasitoids: behavioural and evolutionary ecology. Monographs in Behavior and Ecology. Princeton University Press, Princeton, New Jersey, USA.

Gordon, D. M., R. M. Nisbet, A. Deroos, W. S. C. Gurney, and R. K. Stewart. 1991. Discrete generations in host-parasitoid models with contrasting life-cycles. Journal of Animal Ecology 60:295–308.

Harvey, J. A., I. F. Harvey, and D. J. Thompson. 1994. Flexible larval growth allows use of a range of host sizes by a parasitoid wasp. Ecology 75:1420–1428.

Harvey, J. A., I. F. Harvey, and D. J. Thompson. 2001. Lifetime reproductive success in the solitary endoparasitoid, *Venturia canescens*. Journal of Insect Behavior 14:573–593.

Harvey, J. A., and M. R. Strand. 2002. The developmental strategies of endoparasitoid wasps vary with host feeding ecology. Ecology 83:2439–2451.

Heino, M., and V. Kaitala. 1999. Evolution of resource allocation between growth and reproduction in animals with indeterminate growth. Journal of Evolutionary Biology 12:423–429.

Helm, B. R. 2013. An ontogenetic perspective on the timing of maturation in insects with special consideration of the role of physical and resource thresholds. Dissertation. The University of Arizona, Tuscon, Arizona, USA.

Holling, C. S. 1959. Some characteristics of simple types of predation and parasitism. Canadian Entomologist 91:385–398.

Honek, A. 1993. Intraspecific variation in body size and fecundity in insects: a general relationship. Oikos 66:483–492.

Hoshizaki, D. K., A. G. Gibbs, and N. D. Bond. 2013. Fat body. Pages 132–149 *in* R. F. Chapman, S. J. Simpson, and A. E. Douglas, editors. The insects: structure and function. Cambridge University Press, Cambridge, UK.

Howell, J., and R. C. Fisher. 1977. Food conversion efficiency of a parasitic wasp, *Nemeritis canescens*. Ecological Entomology 2:143–151.

Humphries, M. M., and K. S. McCann. 2014. Metabolic ecology. Journal of Animal Ecology 83:7–19.

Jervis, M. A. 2005. Insects as natural enemies: a practical perspective. Kluwer Academic Publishers, Norwell, Massachusetts, USA.

Jervis, M. A., C. L. Boggs, and P. N. Ferns. 2005. Egg maturation strategy and its associated trade-offs: a synthesis focusing on Lepidoptera. Ecological Entomology 30:359–375.

Jervis, M. A., C. L. Boggs, and P. N. Ferns. 2007. Egg maturation strategy and survival trade-offs in holometabolous insects: a comparative approach. Biological Journal of the Linnean Society 90:293–302.

Jervis, M. A., J. Ellers, and J. A. Harvey. 2008. Resource acquisition, allocation, and utilization in parasitoid reproductive strategies. Annual Review of Entomology 53:361–385.

Jervis, M. A., and P. N. Ferns. 2004. The timing of egg maturation in insects: ovigeny index and initial egg load as measures of fitness and of resource allocation. Oikos 107:449–460.

Jervis, M. A., G. E. Heimpel, P. N. Ferns, J. A. Harvey, and N. A. C. Kidd. 2001. Life-history strategies in parasitoid wasps: a comparative analysis of 'ovigeny'. Journal of Animal Ecology 70:442–458.

Joern, A., and S. T. Behmer. 1997. Importance of dietary nitrogen and carbohydrates to survival, growth, and reproduction in adults of the grasshopper *Ageneotettix deorum* (Orthoptera: Acrididae). Oecologia 112:201–208.

Jonsson, K. I. 1997. Capital and income breeding as alternative tactics of resource use in reproduction. Oikos 78:57–66.

Kaneko, Y., T. Yasanga, M. Suzuki, and S. Sakurai. 2011. Larval fat body cells die during the early pupal stage in the frame of metamorphosis remodelation in *Bombyx mori*. Journal of Insect Physiology 57:1715–1722.

Kearney, M. 2012. Metabolic theory, life history and the distribution of a terrestrial ectotherm. Functional Ecology 26:167–179.

Kearney, M., S. J. Simpson, D. Raubenheimer, and B. Helmuth. 2010*a*. Modelling the ecological niche from functional traits. Philosophical Transactions of the Royal Society B 365:3469–3483.

Kearney, M. R., N. J. Briscoe, D. J. Karoly, W. P. Porter, M. Norgate, and P. Sunnucks. 2010*b*. Early emergence in a butterfly causally linked to anthropogenic warming. Biology Letters 6:674–677.

Kearney, M. R., S. J. Simpson, D. Raubenheimer, and S. Kooijman. 2013. Balancing heat, water and nutrients under environmental change: a thermodynamic niche framework. Functional Ecology 27:950–965.

Kooijman, S. 2013. Waste to hurry: dynamic energy budgets explain the need of wasting to fully exploit blooming resources. Oikos 122:348–357.

Kooijman, S., T. Sousa, L. Pecquerie, J. van der Meer, and T. Jager. 2008. From food-dependent statistics to metabolic parameters, a practical guide to the use of dynamic energy budget theory. Biological Reviews 83:533–552.

Kooijman, S. A. L. M. 2010. Dynamic energy budget theory for metabolic organisation. Cambridge University Press, Cambridge, UK.

Larsen, W. J. 1976. Cell remodelling in the fat body of an insect. Tissue Cell 8:73–92.

Lika, K., S. Augustine, L. Pecquerie, and S. Kooijman. 2014. The bijection from data to parameter space with the standard DEB model quantifies the supply-demand spectrum. Journal of Theoretical Biology 354:35–47.

Lika, K., M. R. Kearney, V. Freitas, H. W. van der Veer, J. van der Meer, J. W. M. Wijsman, L. Pecquerie, and S. Kooijman. 2011*a*. The "covariation method" for estimating the parameters of the standard Dynamic Energy Budget model I: philosophy and approach. Journal of Sea Research 66:270–277.

Lika, K., M. R. Kearney, and S. Kooijman. 2011*b*. The "covariation method" for estimating the parameters of the standard Dynamic Energy Budget model II: properties and preliminary patterns. Journal of Sea Research 66:278–288.

Lika, K., S. A. L. M. Kooijman, and N. Papandroulakis. 2014. Metabolic acceleration in Mediterranean Perciformes. Journal of Sea Research 94:37–46.

Maino, J. L., and M. R. Kearney. 2014. Ontogenetic and interespecific metabolic scaling in insects. American Naturalist 184:695–701.

Maino, J. L., M. R. Kearney, R. M. Nisbet, and S. Kooijman. 2014. Reconciling theories for metabolic scaling. Journal of Animal Ecology 83:20–29.

Mane-Padros, D., J. Cruz, L. Vilaplana, C. Nieva, E. Urena, X. Belles, and D. Martin. 2010. The hormonal pathway

controlling cell death during metamorphosis in a hemimetabolous insect. Developmental Biology 346:150–160.
Mathavan, S., G. Santhi, and B. N. Sethuraman. 1987. Effects of feeding regime on energy allocation to reproduction in the silkworm *Bombyx mori*. Proceedings of the Indian Academy of Sciences, Animal Sciences 96:333–340.
Merkey, A. B., C. K. Wong, D. K. Hoshizaki, and A. G. Gibbs. 2011. Energetics of metamorphosis in *Drosophila melanogaster*. Journal of Insect Physiology 57:1437–1445.
Min, K. J., M. F. Hogan, M. Tatar, and D. M. O'Brien. 2006. Resource allocation to reproduction and soma in *Drosophila*: a stable isotope analysis of carbon from dietary sugar. Journal of Insect Physiology 52:763–770.
Nelliot, A., N. Bond, and D. K. Hoshizaki. 2006. Fat-body remodeling in *Drosophila melanogaster*. Genesis 44:396–400.
Nisbet, R. M., M. Jusup, T. Klanjscek, and L. Pecquerie. 2012. Integrating dynamic energy budget (DEB) theory with traditional bioenergetic models. Journal of Experimental Biology 215:892–902.
Nylin, S., and K. Gotthard. 1998. Plasticity in life-history traits. Annual Review of Entomology 43:63–83.
O'Brien, D. M., D. P. Schrag, and C. M. del Rio. 2000. Allocation to reproduction in a hawkmoth: a quantitative analysis using stable carbon isotopes. Ecology 81:2822–2831.
Ohbayashi, T., K. Iwabuchi, and J. Mitsuhashi. 1994. In-vitro rearing of a larval endoparasitoid, *Venturia canescens* (Gravenhorst) (Hymenoptera, Ichneumonidae). 1. Embryonic development. Applied Entomology and Zoology 29:123–126.
Pecquerie, L., P. Petitgas, and S. Kooijman. 2009. Modeling fish growth and reproduction in the context of the Dynamic Energy Budget theory to predict environmental impact on anchovy spawning duration. Journal of Sea Research 62:93–105.
Raubenheimer, D., S. J. Simpson, and A. H. Tait. 2012. Match and mismatch: conservation physiology, nutritional ecology and the timescales of biological adaptation. Philosophical Transactions of the Royal Society B 367:1628–1646.
Rivero, A., D. Giron, and J. Casas. 2001. Lifetime allocation of juvenile and adult nutritional resources to egg production in a holometabolous insect. Proceedings of the Royal Society B 268:1231–1237.
Rivero, A., and S. A. West. 2002. The physiological costs of being small in a parasitic wasp. Evolutionary Ecology Research 4:407–420.
Roberts, H. L. S., and O. Schmidt. 2004. Lifetime egg maturation by host-deprived *Venturia canescens*. Journal of Insect Physiology 50:195–202.
Roff, D. A. 2002. Life history evolution. Sinauer Associates, Sunderland, Massachusetts, USA.
Rosenheim, J. A., S. J. Jepsen, C. E. Matthews, D. S. Smith, and M. R. Rosenheim. 2008. Time limitation, egg limitation, the cost of oviposition, and lifetime reproduction by an insect in nature. American Naturalist 172:486–496.
Rowe, L., and D. Ludwig. 1991. Size and timing of metamorphosis in complex life-cycles—time constraints and variation. Ecology 72:413–427.
Salt, G. 1976. Hosts of *Nemeretis canescens*, a problem in host specificity of insect parasitoids. Ecological Entomology 1:63–67.
Sequeira, R., and M. Mackauer. 1992. Nutritional ecology of an insect host parasitoid association—the pea aphid *Aphidius ervi* system. Ecology 73:183–189.
Sibly, R. M., and P. Calow. 1986. Physiological ecology of animals: an evolutionary approach. Blackwell Scientific Publications, Oxford, UK.
Simpson, S. J., and D. Raubenheimer. 2012. The nature of nutrition: an unifying framework from animal adaptation to human obesity. Princeton University Press, Princeton, New Jersey, USA.
Spanoudis, C. G., and S. S. Andreadis. 2012. Temperature-dependent survival, development, and adult longevity of the koinobiont endoparasitoid *Venturia canescens* (Hymenoptera: Ichneumonidae) parasitizing *Plodia interpunctella* (Lepidoptera: Pyralidae). Journal of Pest Science 85:75–80.
Stearns, S. C. 1992. The evolution of life histories. Oxford University Press, New York, New York, USA.
Stephens, P. A., I. L. Boyd, J. M. McNamara, and A. I. Houston. 2009. Capital breeding and income breeding: their meaning, measurement, and worth. Ecology 90:2057–2067.
Stevens, D. J., M. H. Hansell, and P. Monaghan. 2000. Developmental trade-offs and life histories: strategic allocation of resources in caddis flies. Proceedings of the Royal Society B 267:1511–1515.
Suzuki, Y., T. Koyama, K. Hiruma, L. M. Riddiford, and J. W. Truman. 2013. A molt timer is involved in the metamorphic molt in *Manduca sexta* larvae. Proceedings of the National Academy of Sciences USA 110:12518–12525.
Taborsky, B. 2006. The influence of juvenile and adult environments on life-history trajectories. Proceedings of the Royal Society B 273:741–750.
Takahashi, F. 1959. The effect of host-finding efficiency of parasites on the cyclic fluctuations of populations in the interacting system of *Ephestia* and *Nemeretis*. Japanese Journal of Ecology 9:88–93.
Tammaru, T., and E. Haukioja. 1996. Capital breeders and income breeders among Lepidoptera—consequences to population dynamics. Oikos 77:561–564.
Tomlinson, S., S. G. Arnall, A. Munn, S. D. Bradshaw, S. K. Maloney, K. W. Dixon, and R. K. Didham. 2014. Applications and implications of ecological energetics. Trends in Ecology and Evolution 29:280–290.
Vet, L. E. M., A. Datema, A. Janssen, and H. Snellen. 1994. Clutch size in a larval pupal endoparasitoid—consequences for fitness. Journal of Animal Ecology 63:807–815.
Wald, G. 1981. Metamorphosis: an overview. Pages 1–39 *in* L. I. Gilbert and E. Frieden, editors. Metamorphosis: a problem in developmental biology. Plenum, New York, New York, USA.
Wessels, F. J., D. C. Jordan, and D. A. Hahn. 2010. Allocation from capital and income sources to reproduction shift from first to second clutch in the flesh fly, *Sarcophaga crassipalpis*. Journal of Insect Physiology 56:1269–1274.
White, E. G., and C. B. Huffaker. 1969. Regulatory processes and population cyclicity in laboratory populations of *Anagasta kühniella* (Zeller) (Lepidoptera: Phycitidae). II. Parasitism, predation, competition and protecting cover. Researches on Population Ecology 11:150–185.
Wissinger, S., J. Steinmetz, J. S. Alexander, and W. Brown. 2004. Larval cannibalism, time constraints, and adult fitness in caddisflies that inhabit temporary wetlands. Oecologia 138:39–47.

Supplemental Material

Ecological Archives

Appendices A and B and Supplements 1 and 2 are available online: http://dx.doi.org/10.1890/14-0976.1.sm